UTILIZATION OF GEOMETRIC SYMMETRIES IN "EDGE" BASED BOUNDARY INTEGRAL EDDY CURRENT SOLUTIONS

Jian-She Wang and Nathan Ida

Department of Electrical Engineering
The University of Akron
Akron, OH 44325, U. S. A.

Abstract - An efficient implementation of the simple layer integral equation procedure for eddy current computation is presented. Vector boundary elements of quadrilateral and trilateral shapes are constructed. These elements, based on "facet" finite elements, have unknowns associated with edges, and are useful for modeling vector surface currents. The simple layer integral procedure is then discretized via the method of moments. A procedure is implemented to fully utilize geometric symmetries of the interior domain. The symmetry planes are not necessarily perfect electric or magnetic conductors. By using symmetric vector shape functions and introducing "symmetric components", the coefficient matrix is symmetrized and then reduced to smaller systems. This procedure is used to compute the eddy current profile of a conducting plate with a small slot.

I. INTRODUCTION

Consider an "externally driven" eddy current problem, where a conductor is excited by an external source, a typical situation in nondestructive testing of conducting materials [1]. Since the problem is unbounded and the conductor is homogeneous, boundary integral procedures are most useful. In particular, we consider here the simple layer integral equation procedure of [2], where only the surface of the conductor needs to be modeled. While a finite element modeling would have to discretize the whole domain, and a volume integral equation modeling would have to discretize the whole conducting region. In [3], the simple layer integral procedure of [2] was implemented using the method of moments [4]. However, the following limitations have been observed. 1) The principal unknowns in the simple layer procedure are the tangential surface layer density functions. The plane triangular vector boundary elements of [5] yield a poor approximation to these tangential functions if the conductor surface is curved. Otherwise a dense boundary mesh will have to be used. It is more efficient and accurate if curvilinear vector boundary elements are used. 2) This method involves a $2N \times 2N$ complex, full matrix, where N is the total number of edges in the boundary element mesh. When it is required to use a very large boundary element mesh, this method needs very large computer resources to fill-in, store and invert the stiffness matrix. In practice, many problems possess, or can be arranged to possess, certain geometric symmetries. These symmetry planes do not have to be electrical walls or magnetic walls, depending on the source configurations and the state variable used. If these symmetries can be utilized, only the principal portion of the problem needs to be considered [6]. This paper addresses these issues. Vector boundary elements of quadrilateral and trilateral shapes are constructed. These elements, based on "facet" finite elements [7,8], have unknowns associated with edges, and are especially suitabe for modeling tangential surface currents. It is possible to establish a boundary element mesh having image symmetry with respect to the geometric symmetry plane(s). Accordingly, the "edge" shape functions and the testing functions are also images with respect to the symmetry plane(s). When these vector functions are used to discretize the coupled integral equations, the symmetry property of the system transfer function is preserved. The global matrix eqaution is then reduced to a number of smaller sub-systems [6]. In the subsequent section, we illustrate details and applications of this procedure.

II. THE SIMPLE LAYER INTEGRAL PROCEDURE

For a conductor under an external excitation, the electric and magnetic fields exterior to its boundary S are determined by the excitation and the outer density functions $(\vec{J}, \rho^e)$; and the fields interior to S by the inner density functions $(\vec{M}, \rho^m)$ [2]. The coupled integral equation formualtion is obtained by requiring the continuity of tangential components of the electric and magnetic fields on the interface S:

$$\vec{E}^{inc}(\vec{r}) \mid_{\tan} = \left\{ j\omega \vec{A}_1(\vec{r}) + \nabla V_1(\vec{r}) - j\omega \vec{A}_2 - \nabla V_2(\vec{r}) \right\} \mid_{\tan}, \quad (1)$$

$$-\vec{H}^{inc}(\vec{r}) \mid_{\tan} = \left\{ \frac{1}{\mu_1} \nabla \times \vec{A}_1(\vec{r}) - \frac{1}{\mu_2} \nabla \times \vec{A}_2(\vec{r}) \right\} \mid_{\tan}, \quad (2)$$

where $\vec{r} \in S$. Potential functions $\vec{A}_1$, $\vec{A}_2$, V_1 andV_2 are defined by

$$\vec{A}_1(\vec{r}) = \mu_1 \iint_S \vec{J}(\vec{r}') \frac{e^{-jk_1 R}}{4\pi R} dS(\vec{r}') \quad (3)$$

$$\vec{A}_2(\vec{r}) = \mu_2 \iint_S \vec{M}(\vec{r}') \frac{e^{-jk_2 R}}{4\pi R} dS(\vec{r}') \quad (4)$$

$$V_1(\vec{r}) = \frac{1}{\epsilon_1'} \iint_S \rho^e(\vec{r}') \frac{e^{-jk_1 R}}{4\pi R} dS(\vec{r}') \quad (5)$$

$$V_2(\vec{r}) = \frac{1}{\epsilon_2} \iint_S \rho^m(\vec{r}') \frac{e^{-jk_2 R}}{4\pi R} dS(\vec{r}') \quad (6)$$

where $R = |\vec{r} - \vec{r}'|$, k_1 and k_2 are wave numbers. The charge densities can be deleted through the following continuity relations

$$\rho^e(\vec{r}') = \frac{-1}{j\omega} \nabla_S' \bullet \vec{J}(\vec{r}') \quad \rho^m(\vec{r}') = \frac{-1}{j\omega} \nabla_S' \bullet \vec{M}(\vec{r}'). \quad (7)$$

Since the surface outer layer density $\vec{J}$ and inner layer density $\vec{M}$ are defined on a surface, they may be treated as the special case of *form*-II vectors. These functions can be best approximated via tangential, vector expansion functions $\vec{f}_n$:

$$\vec{J}(\vec{r}') = \sum_{n=1}^{N} J_n \vec{f}_n(\vec{r}'), \qquad \vec{M}(\vec{r}') = \sum_{n=1}^{N} M_n \vec{f}_n(\vec{r}') \quad (8)$$

where the coefficients J_n and M_n stand for the transverse components of the outer layer-density and inner layer-density associated with the n-th common edge. Construction of these functions is given in the next section. To determine these coefficients, the coupled integral equations are tested using the method of moments [4] and the following symmetric product:

Manuscript received July 7, 1991

$$< \vec{\mathbf{f}}, \vec{\mathbf{g}} > = \iint_S \vec{\mathbf{f}} \bullet \vec{\mathbf{g}} dS. \tag{9}$$

A partitioned matrix equation is obtained:

$$\begin{bmatrix} Z^{JJ} & Z^{JM} \\ Z^{MJ} & Z^{MM} \end{bmatrix} \begin{bmatrix} J \\ M \end{bmatrix} = \begin{bmatrix} E^{inc} \\ H^{inc} \end{bmatrix}. \tag{10}$$

The above equation is dense and non-symmetric.

III. VECTOR BOUNDARY ELEMENTS

In this section, we construct vector boundary elements of curvilinear quadrilateral and trilateral shapes. Tangential vector fields defined on a surface, resemble form-II vector fields. "Facet" finite elements [7,8] are suitable for approximating form-II vector fields. Thus, a vector boundary element is obtained by allowing the height of a "facet" element (curvilinear haxahedral or tetrahedral shape) to tend to zero [9]. While a "facet" element is associated with facets, a vector boundary element is associated with edges. Since the Jacobian is zero, the normalization must be changed. Let the vector shape functions be of the following form:

$$\vec{\mathbf{f}}_i(\vec{\mathbf{r}}) = \psi_i(\xi, \eta)\vec{\mathbf{u}}_i(\vec{\mathbf{r}}), \quad i = 1, \cdots, M_b, \tag{11}$$

where M_b is the number of unknowns in the boundary element. For an edge with a direction vector $\hat{\mathbf{e}}$, the transverse direction $\hat{\tau}$ of that edge is defined as the normal direction of the plane formed by $\hat{\mathbf{e}}$ and $\hat{\mathbf{n}}$. The basic strategy for constructing vector shape functions is to:

- use a nodal shape function as ψ_i. It has been normalized such that it equals 1 at node i and zero at other nodes;
- choose $\vec{\mathbf{u}}_i$ along the parametric direction, so that the surface current is flowing out of the element through the edge on which node i resides;
- normalize $\vec{\mathbf{u}}_i$, such that its projection in the transverse direction $\hat{\tau}$ is 1 at node i. Therefore, the transverse component of the surface current flowing past the edge is continuous; no line charges are present.

If a surface flow $\vec{\mathbf{J}}_s$ is expanded as

$$\vec{\mathbf{J}}_s(\vec{\mathbf{r}}) = \sum_{i=1}^{M} \mathcal{J}_i \vec{\mathbf{f}}_i(\vec{\mathbf{r}}), \tag{12}$$

$\mathcal{J}_i$ is the transverse component of $\vec{\mathbf{J}}_s$ at node i flowing past the edge where node i resides in.

Consider first a curvilinear quadrilateral shape shown in Fig. 1. The geometric parametrization is given by

$$\vec{\mathbf{r}} = \sum_{j=1}^{N} N_j(\xi, \eta)\vec{\mathbf{r}}_j, \tag{13}$$

where $N_j(\xi, \eta)$ are the shape functions of a nodal element, N is the number of nodes in the element, and $\vec{\mathbf{r}}_j$ are the corresponding postition vectors. The parametric directions are

$$\vec{\mathbf{V}}_\xi = \frac{\partial \vec{\mathbf{r}}}{\partial \xi}, \quad \vec{\mathbf{V}}_\eta = \frac{\partial \vec{\mathbf{r}}}{\partial \eta}. \tag{14}$$

The cross product of these two vectors, upon normalization, provides the surface normal $\hat{\mathbf{n}}$. Let the transverse directions for parametric lines along ξ and η directions be $\hat{\tau}_\xi$ and $\hat{\tau}_\eta$, respectively. The direction vectors for edges in ξ and η directions are chosen as

$$\vec{\mathbf{u}}_i = \pm \frac{\vec{\mathbf{V}}_\xi}{\hat{\tau}_\xi \cdot \vec{\mathbf{V}}_\xi} \quad \text{and} \quad \vec{\mathbf{u}}_i = \pm \frac{\vec{\mathbf{V}}_\eta}{\hat{\tau}_\eta \cdot \vec{\mathbf{V}}_\eta}. \tag{15}$$

These vectors provide a continuous transverse component. Since there are two parametric lines intersecting an internal point, two vector shape functions are defined.

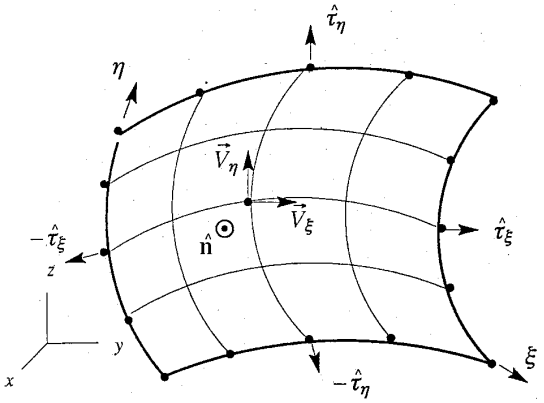

Fig.1 A Curvilinear Quadrilateral Boundary Element.

Consider now a curvilinear trilateral shape shown in Fig.2. The geometric parametrization is given by

$$\vec{\mathbf{r}} = \sum_{j=1}^{N} N_j(L_1, L_2, L_3)\vec{\mathbf{r}}_j. \tag{16}$$

For each corner node $k = 1, 2, 3$, two parametric directions $\vec{\mathbf{V}}_{k,i}$, $i = 1, 2, 3$, $i \neq k$, can be defined. These two vectors provide the normal direction $\hat{\mathbf{n}}$. Now consider edge $e_{3,1}$. The transverse direction $\hat{\tau}_2$ is formed by the cross product of $\hat{\mathbf{n}}$ and $\vec{\mathbf{V}}_{3,1}$. Again, we allow the current flow along parametric lines. Since there are two sets of parametric lines intersecting edge $e_{3,1}$, we choose

$$\vec{\mathbf{u}}_i = \left[(1 - \xi_i) \frac{\vec{\mathbf{V}}_{2,3}}{\hat{\tau}_2 \cdot \vec{\mathbf{V}}_{2,3}} + \xi_i \frac{\vec{\mathbf{V}}_{2,1}}{\hat{\tau}_2 \cdot \vec{\mathbf{V}}_{2,1}} \right], \tag{17}$$

for any node i on $e_{3,1}$. Vector shapes for nodes on other edges can be obtained by symmetry. Since there are three parametric lines intersecting an internal node, three vector shape functions are defined.

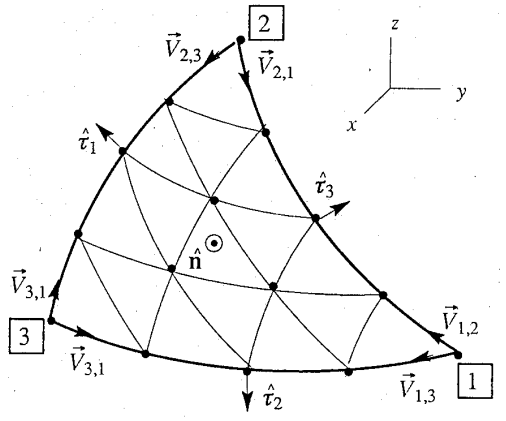

Fig.2 A Curvilinear Trilateral Boundary Element.

Quasi elements are frequently used, where each edge has one degree of freedom, since the transverse component is constant along the edge [5]. To use the proposed boundary elements in the integral equation procedure, the surface divergence needs to be computed. Using the fundamental definition of surface divergence, it is found that the surface divergence associated with equation (15) in a quadrilateral element is

$$\nabla_S \cdot \vec{\mathbf{f}}_i = \pm \frac{|\vec{\mathbf{V}}_\eta|}{|\vec{\mathbf{V}}_\xi \times \vec{\mathbf{V}}_\eta|} \frac{\partial \psi_i}{\partial \xi} \quad \text{and} \quad \pm \frac{|\vec{\mathbf{V}}_\xi|}{|\vec{\mathbf{V}}_\xi \times \vec{\mathbf{V}}_\eta|} \frac{\partial \psi_i}{\partial \eta}. \tag{18}$$

The surface divergence of the boundary element shape function associated with equation (17) in a trilateral element is

$$\nabla_S \cdot \vec{\mathbf{f}}_i = \frac{(1-\xi_i)|\vec{\mathbf{V}}_{2,1}|}{|\vec{\mathbf{V}}_{2,3} \times \vec{\mathbf{V}}_{2,1}|} \left(\frac{\partial \phi_i}{\partial L_1} - \frac{\partial \phi_i}{\partial L_3} \right) + \frac{\xi_i |\vec{\mathbf{V}}_{1,2}|}{|\vec{\mathbf{V}}_{1,2} \times \vec{\mathbf{V}}_{1,3}|} \left(\frac{\partial \phi_i}{\partial L_2} - \frac{\partial \phi_i}{\partial L_3} \right). \tag{19}$$

The singular integral in an element can be resolved using Taylor expansions and semi-analytical integration [10].

IV. UTILIZATION OF SYMMETRIES

If the solution domain has some sort of symmetry, the redundant computation associated with (10) can be condensed. Consider first a one-way symmetry problem. Let $x = 0$ be the symmetry plane (see the upper portion of Fig.3), with the region $x > 0$ denoted by a subscript "I", and the region $x < 0$ by a subscript "II". These two portions are discretized by two boundary element meshes which are symmetric with respect to $x = 0$. Orientations of edges in region "II" are images of the edges in region "I". For the n-th edge in region "I" and its image in region "II", the corresponding vector shape function $\vec{\mathbf{f}}_{n,\mathrm{II}}$ is the image of $\vec{\mathbf{f}}_{n,\mathrm{I}}$. With the basis functions so defined, the following partitioned matrix equation is obtained:

$$\begin{bmatrix} Z_{\mathrm{I,I}} & Z_{\mathrm{I,II}} \\ Z_{\mathrm{II,I}} & Z_{\mathrm{II,II}} \end{bmatrix} \begin{bmatrix} I_{\mathrm{I}} \\ I_{\mathrm{II}} \end{bmatrix} = \begin{bmatrix} V_{\mathrm{I}} \\ V_{\mathrm{II}} \end{bmatrix}, \tag{20}$$

where each submatrix corresponds to a partitioned submatrix; for example,

$$Z_{\mathrm{I,II}} = \begin{bmatrix} Z_{\mathrm{I,II}}^{JJ} & Z_{\mathrm{I,II}}^{JM} \\ Z_{\mathrm{I,II}}^{MJ} & Z_{\mathrm{I,II}}^{MM} \end{bmatrix}, \quad I_{\mathrm{I}} = \begin{bmatrix} J_{\mathrm{I}} \\ M_{\mathrm{I}} \end{bmatrix}, \quad V_{\mathrm{I}} = \begin{bmatrix} E_{\mathrm{I}}^{\mathrm{inc}} \\ H_{\mathrm{I}}^{\mathrm{inc}} \end{bmatrix}. \tag{21}$$

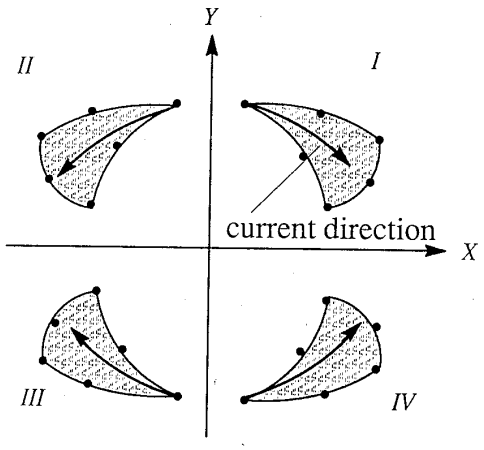

Fig.3 Constructing Symmetric Boundary Elements (Two Symmetric Planes).

It can be shown that $Z_{\mathrm{I,I}} = Z_{\mathrm{II,II}}$, $Z_{\mathrm{I,II}} = Z_{\mathrm{II,I}}$ (i.e., the vector potentials and the principal value integrals are image-symmetric, and the scalar potential terms are equal). Therefore, equation (20) is block symmetrized. It can be reduced to two decoupled, smaller subsystems by introducing new variables $\tilde{I}_{\mathrm{I}}$ and $\tilde{I}_{\mathrm{II}}$ [6]:

$$[Z_{\mathrm{I,I}} + Z_{\mathrm{I,II}}]\{\tilde{I}_{\mathrm{I}}\} = \{V_{\mathrm{I}} + V_{\mathrm{II}}\} \tag{22}$$

$$[Z_{\mathrm{I,I}} - Z_{\mathrm{I,II}}]\{\tilde{I}_{\mathrm{II}}\} = \{V_{\mathrm{I}} - V_{\mathrm{II}}\}. \tag{23}$$

The actual currents are obtained through:

$$\{I_{\mathrm{I}}\} = 1/2\{\tilde{I}_{\mathrm{I}} + \tilde{I}_{\mathrm{II}}\} \qquad \{I_{\mathrm{II}}\} = 1/2\{\tilde{I}_{\mathrm{I}} - \tilde{I}_{\mathrm{II}}\}. \tag{24}$$

In fact, one may view $\tilde{I}_{\mathrm{I}}$ as the symmetric components, $\tilde{I}_{\mathrm{II}}$ as the anti-symmetric components. The classification of these two components does not rely on the source distribution. The actual current is the superposition of the two components. If the source is symmetrically distributed, $V_{\mathrm{I}} = V_{\mathrm{II}}$, the anti-symmetric components vanish, and $I_{\mathrm{I}} = \tilde{I}_{\mathrm{I}} = I_{\mathrm{II}}$. From (22), it can be seen that, the filling-in computation is reduced by a factor of 2, and the inverting computation by a factor of 4. A peculiarity arises when an edge lies on the symmetry plane. Since $\tilde{I}_{\mathrm{I}}$ is symmetric with respect to the symmetry plane, the transverse component across the edge must be zero. Equation (23) should be modified accordingly.

For a geometrical shape possessing two symmetry planes (for example, $x = 0$ and $y = 0$), the four quadrants are denoted by "I" to "IV", respectively, as shown in Fig.3. Following the idea used before, it is possible to construct triangular meshes and basis functions which are images with respect to the planes $x = 0$ and $y = 0$. The following matrix equation is obtained:

$$\begin{bmatrix} Z_{\mathrm{I,I}} & Z_{\mathrm{I,II}} & Z_{\mathrm{I,III}} & Z_{\mathrm{I,IV}} \\ Z_{\mathrm{II,I}} & Z_{\mathrm{II,II}} & Z_{\mathrm{II,III}} & Z_{\mathrm{II,IV}} \\ Z_{\mathrm{III,I}} & Z_{\mathrm{III,II}} & Z_{\mathrm{III,III}} & Z_{\mathrm{III,IV}} \\ Z_{\mathrm{IV,I}} & Z_{\mathrm{IV,II}} & Z_{\mathrm{IV,III}} & Z_{\mathrm{IV,IV}} \end{bmatrix} \begin{bmatrix} I_{\mathrm{I}} \\ I_{\mathrm{II}} \\ I_{\mathrm{III}} \\ I_{\mathrm{IV}} \end{bmatrix} = \begin{bmatrix} V_{\mathrm{I}} \\ V_{\mathrm{II}} \\ V_{\mathrm{III}} \\ V_{\mathrm{IV}} \end{bmatrix}. \tag{25}$$

It can be shown that only four submatrices in equation (25) are independent. Thus, (25) can be decoupled into four subsystems:

$$[Z_{\mathrm{I,I}} + Z_{\mathrm{I,II}} + Z_{\mathrm{I,III}} + Z_{\mathrm{I,IV}}]\{\tilde{I}_{\mathrm{I}}\} = \{V_{\mathrm{I}} + V_{\mathrm{II}} + V_{\mathrm{III}} + V_{\mathrm{IV}}\} \tag{26}$$

$$[Z_{\mathrm{I,I}} - Z_{\mathrm{I,II}} + Z_{\mathrm{I,III}} - Z_{\mathrm{I,IV}}]\{\tilde{I}_{\mathrm{II}}\} = \{V_{\mathrm{I}} - V_{\mathrm{II}} + V_{\mathrm{III}} - V_{\mathrm{IV}}\} \tag{27}$$

$$[Z_{\mathrm{I,I}} + Z_{\mathrm{I,II}} - Z_{\mathrm{I,III}} - Z_{\mathrm{I,IV}}]\{\tilde{I}_{\mathrm{III}}\} = \{V_{\mathrm{I}} + V_{\mathrm{II}} - V_{\mathrm{III}} - V_{\mathrm{IV}}\} \tag{28}$$

$$[Z_{\mathrm{I,I}} - Z_{\mathrm{I,II}} - Z_{\mathrm{I,III}} + Z_{\mathrm{I,IV}}]\{\tilde{I}_{\mathrm{IV}}\} = \{V_{\mathrm{I}} - V_{\mathrm{II}} - V_{\mathrm{III}} + V_{\mathrm{IV}}\}. \tag{29}$$

Similarly, $\tilde{I}_{\mathrm{I}}$ is a component symmetric to both $x = 0$ and $y = 0$, $\tilde{I}_{\mathrm{II}}$ is a component anti-symmetric to both planes, $\tilde{I}_{\mathrm{III}}$ and $\tilde{I}_{\mathrm{IV}}$ are component symmetric to one plane but anti-symmetric to another plane. The actual currents are

$$\{I_{\mathrm{I}}\} = 1/4\{\tilde{I}_{\mathrm{I}} + \tilde{I}_{\mathrm{II}} + \tilde{I}_{\mathrm{III}} + \tilde{I}_{\mathrm{IV}}\} \qquad \{I_{\mathrm{II}}\} = 1/4\{\tilde{I}_{\mathrm{I}} - \tilde{I}_{\mathrm{II}} + \tilde{I}_{\mathrm{III}} - \tilde{I}_{\mathrm{IV}}\} \tag{30}$$

$$\{I_{\mathrm{III}}\} = 1/4\{\tilde{I}_{\mathrm{I}} + \tilde{I}_{\mathrm{II}} - \tilde{I}_{\mathrm{III}} - \tilde{I}_{\mathrm{IV}}\} \qquad \{I_{\mathrm{IV}}\} = 1/4\{\tilde{I}_{\mathrm{I}} - \tilde{I}_{\mathrm{II}} - \tilde{I}_{\mathrm{III}} + \tilde{I}_{\mathrm{IV}}\}. \tag{31}$$

By solving (26)-(29), the filling-in computation is reduced by a factor of 4, and the inverting computation by a factor of 16.

Without too much difficulty, the same idea can be extended to problems with three-way symmetries. The filling-in computation can be reduced by a factor of 8, and the inverting computation by a factor of 64. Field integration over surface sources should be done over the entire surface S.

V. NUMERICAL EXAMPLES

To verify that this procedure is correct, the problem of a sphere in a uniform alternating field is considered using three symmetry planes. The sphere has a radius $a = 1m$. The incident frequency is $10kHz$ and the conductivity is $10^3\mho/m$. Fig.4 shows the distribution of the B_z component on the x-z plane for $z = 1.1m$ to $z = 2.0m$. These curves compare well with analytical solutions.

Consider now a conducting plate with a slot under a uniform alternating field. One quarter of the structure is shown in Fig.5, where $A = B = C = 1.0m$, $a = b = c = 0.2m$. The incident frequency is $10kHz$ and the conductivity is $10^3\mho/m$. Two symmetry planes can be used in this problem. Fig.6 shows the distribution of the B_z component on the x-z plane for $z = 1.1$ to $z = 2.0$.

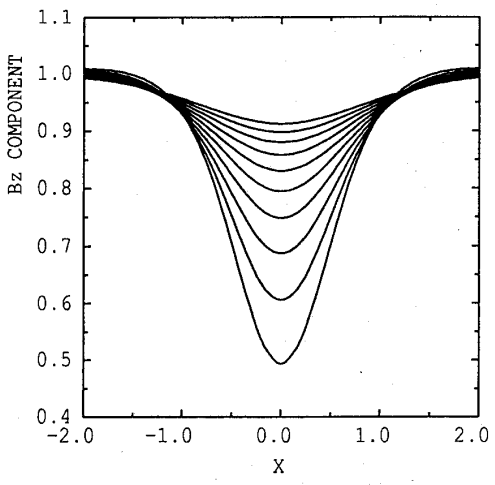

Fig.4 A Conducting Sphere in an Alternating Field: B_z Component on the x-z Plane.

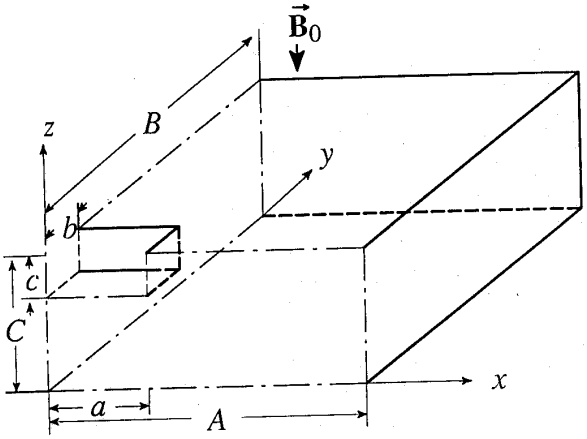

Fig.5 A Conducting Plate with a Small Slot.

VI. CONCLUSIONS

"Edge" based boundary elements, similar to "facet" finite elements, were constructed. These boundary elements were extremely suitable for the method of moments solution of boundary integral equations with tangential density functions as unknowns. By constructing symmetric boundary elements, geometric symmetries were fully utilized. Although the procedure was presented using a single conductor, it applies to mutiple conductors and layered structure as well.

ACKNOWLEDGMENT

This work was supported in part by NSF Grant #EET8714628 and in part by The Ohio Board of Regents Academic Challenge Program. Computational Resources on the Ohio Supercomputer Center CRAY Y-MP are gratefully acknowledged.

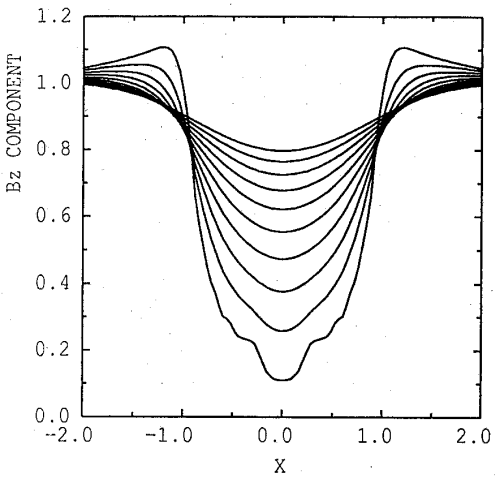

Fig.6 B_z Component on the x-z plane.

REFERENCES

[1] W. Lord, "Applications of Numerical Field Modeling to Electromagnetic Methods of Nondestructive Testing", IEEE Trans. Magnetics, Vol. MAG-19, No.6, 1983, pp. 2437 - 2442.

[2] R. C. MacCamy and E. Stephan, "Solution Procedure for Three-Dimensioanl Eddy Current Problems", J. Math. Anal. Appl., Vol. 101, 1984, pp. 348 - 379.

[3] Jian-She Wang and Nathan Ida, "3D Finite Element Calculation of Harmonic Electromagnetic Fields", IEEE Trans. Magnetics, Vol. 26, No.2, 1990, pp. 654 - 657.

[4] R. F. Harrington, Field Computation by Moment Methods, The Macmillan Company, New York, 1968.

[5] S. M. Rao, D. R. Wilton and A. W. Glisson, "Electromagnetic Scattering by Surfaces of Arbitrary Shape", IEEE Trans. Antennas Propagat., Vol. AP-30, No.3, 1982, pp. 409 - 418.

[6] Chang-Yu Wu and D. K. Cheng, "A Method for Symmetrizing Generalized Impedance Matrices", IEEE Trans. Electromagnetic Compartibility, Vol. EMC-19, No.2, 1977, pp. 81 - 88.

[7] J. C. Nedelec, "Mixed Finite Elements in $\Re^3$", Numerische Mathematik, Vol.35, pp. 315 - 341, 1980.

[8] A. Bossavit, "Whitney forms: a Class of Finite Elements for Three-Dimensional Computations in Electromagnetism", IEE Proc., Vol.135, Pt.A, No.8, pp.493 - 500, 1988.

[9] J. S. van Welij, "Calculation of Eddy Currents in terms of H on Hexahedra",IEEE Trans. Magnetics, Vol.MAG-21, No.6, pp. 2239 - 2241, 1985.

[10] M. H. Aliabadi, W. S. Hall and T. G. Phemister, "Taylor Expansions for Singular Kernels in the Boundary Element Method" Int. J. Numer. Meth. Engr., Vol.21, 1985, pp. 2221 - 2236.